RSC Advances

Evaluation of the Yasuda parameter on atmospheric plasma deposition of allyl methacrylate

Alexandros Kakaroglou [*1], Bernard Nisol[2], Kitty Baert[1], Iris De Graeve[1], François Reniers[2], Guy Van Assche[3], and Herman Terryn[1]

[1]Research Group Electrochemical and Surface Engineering (SURF), Department of Materials and Chemistry (MACH), Vrije Universiteit Brussel, Pleinlaan 2, 1050 Brussels, Belgium

[2]Faculty of Sciences - Analytical and Interfacial Chemistry, Universitè Libre de Bruxelles, 1050 Brussels, Belgium

[3]Research Group Physical Chemistry and Polymer Science (FYSC), Department of Materials and Chemistry (MACH), Vrije Universiteit Brussel, Pleinlaan 2, 1050 Brussels. Belgium

February 23, 2015

Abstract

This work studies the influence of proportional change in discharge power and the monomer feed on the morphology and the chemistry of atmospheric plasma deposited films. Atmospheric plasma coatings of allyl methacrylate were deposited using a dielectric barrier discharge plasma under different conditions but always

[*]akakarog@vub.ac.be

1

under the same ratio between discharge power and monomer feed (W/FM). It is shown that a constant W/FM does not necessarily provide the same chemistry and the same morphology in atmospheric pressure plasma. This is explained since the higher discharge power of the plasma results in an increase of streamers altering the distribution of energy among the plasma species. On the surface of the deposited coatings, globular-like features were observed which are suggested to be formed in the volume of the discharge. The deposition rate is also influenced providing thicker coatings when high monomer feed/high power are used. Finally, infrared spectra showed a higher retention of the ester functionality at high power/high monomer feed.

1   Introduction

The importance of the properties of material surfaces in the industry increased the interest for novel surface treatment processes. Plasma treatments are already used to modify the surface properties in several technological fields such as textiles, microelectronics, automotive, and aerospace industry.[1–4] The recent development of non-thermal atmospheric plasmas created new perspectives in the industrial use of plasma treatments.[5–7]

Plasma polymerization is a plasma process which is used for the deposition of organic films on various substrates. These films provide several surface properties like improved adhesion, protection of the substrate from the environment or enhanced the hydrophillicity of the surface.[8,9]

A proposed parameter used for tuning the plasma polymerization is the W/FM ratio, known also as Yasuda parameter in low pressure plasma, where W is the power of the discharge, F and M are the flow rate and the molecular weight of the precursor respectively.[10] W/FM has been considered to be an important parameter of plasma the polymerization process; low W/FM values result in less fragmentation of the precursor and increase the probability to retain functionalities while higher values provoke a more plasma-state polymerization.

W/FM may provide a first estimation about the initial plasma deposition parameters, however its use has been questioned as it cannot be used to transfer deposition

parameters to different experimental setups in low-pressure atmospheric plasmas.[11,12] Apart from its extensive use in low-pressure plasma polymerization, W/FM is currently used by several research groups as deposition parameter in atmospheric pressure plasma polymerization[13–21] where the precursor is diluted in an inert gas. The use of Yasuda parameter in this context provides information about the amount of energy that is necessary to polymerize the precursor, however it should be highlighted that this parameter is originally intended to be used only in low pressure plasmas where the precursor was not mixed with an inert gas.[12]

In this work, allyl methacrylate (AMA) was deposited by means of an atmospheric plasma Dielectric Barrier Discharge (DBD). The discharge power and the monomer feed were proportionally changed, keeping the W/FM parameter constant, and the morphology, the thickness and the chemistry of the deposited coatings were studied. This preliminary work challenges the use of the W/FM parameter as is in atmospheric plasma, by several authors,[13–21] including the present authors and opens new lines of inquiry, in the further study of plasma parameters at atmospheric pressure.

2 Experimental

2.1 Materials

The coatings were deposited on a AA2024-T3 aluminium alloy supplied by Thyssen-Krupp Aerospace. Substrates were cut to $40 \times 50 \, \text{mm}$. AMA of $\geq 98\%$ purity was obtained from Sigma-Aldrich (CAS No: 96-05-9) and used as precursor for the plasma deposition. Prior to the deposition, substrates were mechanically polished up to 1800 grit to reduce the roughness and reveal a fresh surface. Their surface was then cleaned with acetone and ethanol. Argon of $99.99 \, \%$ purity was used as plasma gas.

2.2 Plasma reactor

A home-made DBD reactor was used for the deposition of the coatings. Figure 1 shows a representation of the deposition reactor. In this reactor, the bottom electrode
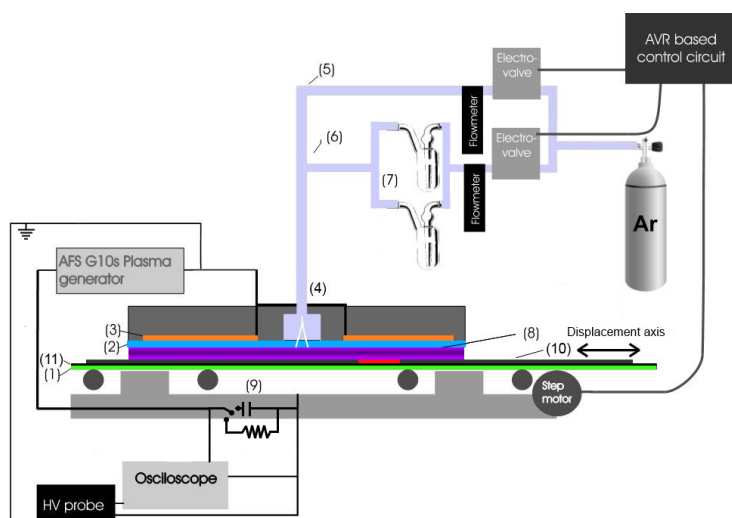
Figure 1: Schematic representation of the plasma DBD reactor.

(1-green) is a long aluminum plate covered with a glass (11-black) which is used as dielectric. The substrates (8-red) are placed on top of this glass. The bottom electrode can move along the top electrode which results to the displacement of the substrates inside and outside the discharge. That results to a homogeneous treatment or covering of the substrates along the displacement axis (see fig. 1). Two large plates (10-grey) of the same material and thickness with the substrate were placed in both sides to avoid changes in the discharge due to the absence of substrate in the plasma gaps. Two copper plates (3-orange) were used as top electrodes and in the middle the gas/precursor inlet (4) was placed. A borosilicate glass (2-tyrqoise) was used as dielectric of the top electrode. In order to introduce the precursor in the discharge, a part of the flow (6) was diverted through two bubblers both containing the precursor (7). By controlling this flow, the monomer feed was also controlled. A sinusoidal voltage with frequency at 17.1 kHz was applied to the top electrode by means of an AFS-G10S power generator. The bottom electrode was connected to the ground.

2.3 Plasma deposition

Prior to each deposition, the plasma reactor was cleaned thoroughly using acetone and ethanol. The deposition started by flushing the reactor with at least 12 slm of Ar for

4

15 s and igniting the Ar discharge without any precursor. The substrates were initially treated by argon plasma for one pass, i.e. a full displacement of the bottom electrode from one side of the reactor to the other and then back, in order to clean and activate the substrate. Then with three passes of plasma deposition were performed. The speed of the bottom electrode was adjusted so that each point of the substrate would remain in the discharge for 50 s in every pass. The total flow of argon during the deposition was 20 slm and the flow rate that was diverted through the bubblers to achieve a certain monomer feed.

The knowledge of the exact discharge power was necessary for the accurate calculation of the W/FM parameter. For this reason, the power consumed in the discharge was calculated. It is known from the literature that the energy consumed per discharge cycle (E_p) is equal to the area of the closed loop of the voltage between the two electrodes of the capacitor (V_d) versus the charge crossing the capacitor (Q). The average consumed discharge power (W_c) was then calculated by dividing the E_p with the period of the discharge cycle.[22–24] A high voltage probe connected between the top electrode and the ground was used to record the V_d. The determination of the Q was done by measuring the voltage (V_q) between the two plates of a capacitor ($C_q =0.01\,\mu F$) connected between the bottom electrode and the ground.

$$Q(t) = V_q C_q \tag{1}$$

The consumed energy per cycle is calculated by the following formula:

$$E_c = f \oint Q(t)dV_d \tag{2}$$

where f is the frequency of the discharge(17.1 kHz),

The flow rate was adjusted in order to obtain equal W/FM in all depositions. The monomer feed (FM) was calculated based on the weight difference of the bubblers before and after each deposition.[20] The current was estimated by measuring the volatage drop in a 10 Ω resistor which was connected in series with the plasma reactor (see fig. 1).

5

3 Morphological characterization techniques

High resolution electron images of the deposited coatings were acquired by means of a Scanning Electron Microscope (SEM) JEOL JSM-7000F) for morphological study. Samples were coated with a 2 nm Pt/Pd coating to avoid charge accumulation. Images of x10000 and x100000 magnification were acquired at an accelerating voltage of 10 kV and a working distance of 10 mm.

Figure 2: Schematic representation of the model used in the SE.

The thickness of the coatings was estimated by Spectroscopic Ellipsometry (SE). Measurements were performed with a J. Woollam M-2000 variable angle spectroscopic ellipsometer. The spectra were acquired at an angle of $70°$ within the range of 245 nm to 998.6 nm. For the interpretation of the ellipsometric data, an optical model based on the morphology observed by Scanning Electron Microscopy (SEM) that contains the optical parameters of various sublayers was used. It consisted of an aluminum substrate,[25] an Al_2O_3 layer,[26] a compact Cauchy film in which the presence of voids was not taken into consideration and a Cauchy film mixed with empty space on top was used. The Al_2O_3 had a fixed thickness at 10 nm, the Cauchy film was used to model the compact part of the plasma polymer and the mixed film was used to model the surface roughness or porosity. For the latter, a Bruggeman effective medium approximation (EMA) model was used of the Cauchy layer with empty space.[27,28] Figure 2 shows a schematic representation of the optical model. The thickness of the compact and rough layers and the percentage of empty space in the latter were fitted by minimizing the Mean Square Error (MSE).

Atomic Force Microscopy (AFM) was also used for the study of the surface morphology of the coatings. An XE-100 apparatus from PARK systems was used in non-contact mode for recording 5×5 μm surface mappings.

6

4   Chemical characterization techniques

Infrared spectra were recorded with a Nicolet 6700 FTIR spectrometer (Thermo) with a diamond crystal single bounce Attenuated Total Reflectance (ATR) setup. The crystal had circular surface of 1.5 mm diameter in which the measured area was exposed. All FTIR spectra were acquired with a $4\,\text{cm}^{-1}$ resolution, 64 scans and a $45°$ of incidence. Data analysis was performed using OMNIC (version 8.1).

Raman spectra were recorded with a LabRAM HR Evolution (Horiba Scientific) confocal Raman microscope. In all experiments, the 532 nm wavelength of a solid state laser with an incident power of 1 mW was focused through an x100 objective on the surface of the samples. The scattered light was collected by the same objective to a multichannel air cooled CCD detector (spectral resolution $< 1\,\text{cm}^{-1}$).

5   Results and discussion
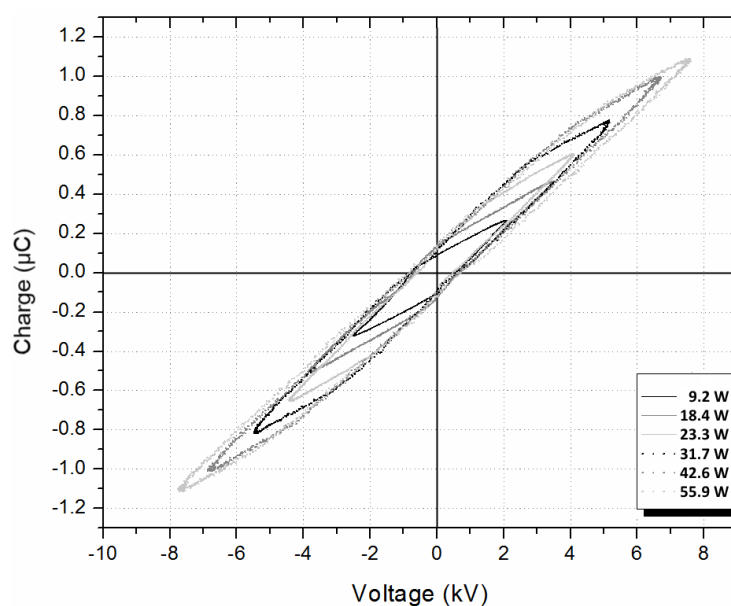

Figure 3: V-Q Lissajous curves for six different powers.

Figure 3 shows the V-Q Lissajous curves for six different output powers (W_o) and table 1 shows the estimated W_c. The W/FM parameter in all depositions had a value

Table 1: Estimated W/FM in MJ$\cdot$kg^{-1}.

W_o	W_c	Flow rate	FM	W/FM
10 W	9.2 W	1 slm	30 mg$\cdot$min^{-1}	18.4
20 W	18.4 W	2 slm	60 mg$\cdot$min^{-1}	18.4
30 W	23.3 W	3 slm	84 mg$\cdot$min^{-1}	16.6
40 W	31.7 W	4 slm	100 mg$\cdot$min^{-1}	19.0
60 W	42.6 W	6 slm	140 mg$\cdot$min^{-1}	18.3
80 W	55.9 W	8 slm	200 mg$\cdot$min^{-1}	16.8

near 17.7 ± 0.8 MJ$\cdot$kg^{-1}. These values are considerably lower compared to the values estimated in previous depositions of AMA.[20,29,30] The difference in the nature between the low and the high power could be also macroscopically observed as in discharge powers above 31.7 W, a considerable amount of streamers was appearing while at lower powers streamers appeared only at the edges of the substrates. At low powers, the V-Q Lissajous curves exhibit a parallelogram shape while at higher powers their edges are slightly deformed, indicating the presence of some residual charge carriers at all times.[31] While a certain power is essential to maintain an atmospheric pressure glow discharge, higher power, and subsequently higher current density, is expected to induce a transition to a filamentary discharge.[32,33] Indeed, as confirmed by the current measurements (see fig. 4), higher discharge powers result to a more filamentary discharge. There is an obvious transition to filamentary mode between 18.4 W and 23.3 W. Therefore, the presence of filaments affects the local current density in the discharge and energy distribution among the excited species.

5.1 Morphological study

SEM was used for the evaluation of the morphology of the deposited coatings. Figure 5 shows the images of the deposited coatings and the substrate for comparison. In all cases, the images show a total coverage of the substrate. In the surface of all coatings, some 'globular'-like features were present. Those features, which were modeled as a rough layer in SE are products coming from the polymerization in the volume of the discharge. Plasma-produced radicals originating from the initial monomer are recombined in the volume of the discharge, forming sub-micron particles which are
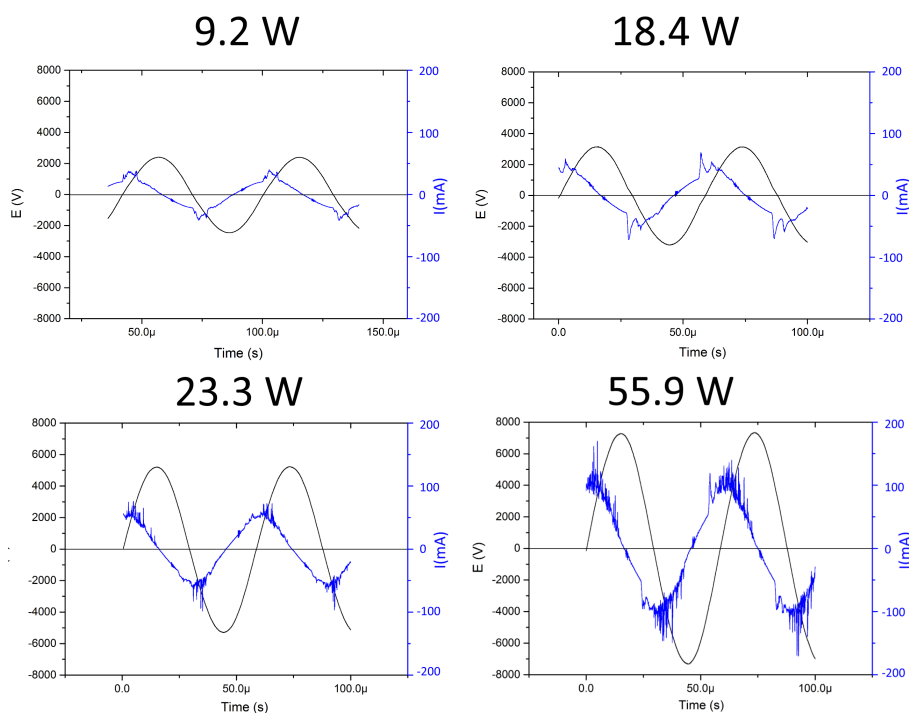
9.2 W

18.4 W

23.3 W

55.9 W

Figure 4: *V* (black) and *dQ/dt* (blue) waveforms for three different powers: 9.2 W, 31.7 W and 55.9 W.

then depositing on the substrate. The formation of such particles has been already mentioned in the deposition of silanes.[34–37] At low power and low monomer feeds (9 W), these features are smaller and less dense while when the power increases (18 W, 31.7 W and 42.6 W), they become denser and larger. At 55.9 W, they are incorporated into the coating. In the high magnification images of fig. 6, the difference in the size of those particles is more evident. This difference in the morphology of the surface of the coatings indicates a change in the formation mechanism of the plasma polymers. The increase in the discharge current and the monomer flow are expected to influence the density, the mean free path of the excited species and consequently the type of the discharge. That would explain a different growth mechanism, in which polymerization in the volume of the discharge is favored at higher powers relative to interactions at the discharge-substrate interface.

The morphology of the coatings was verified by AFM. Figure 7 shows the topo-logical images of the coatings deposited with different conditions. In agreement with
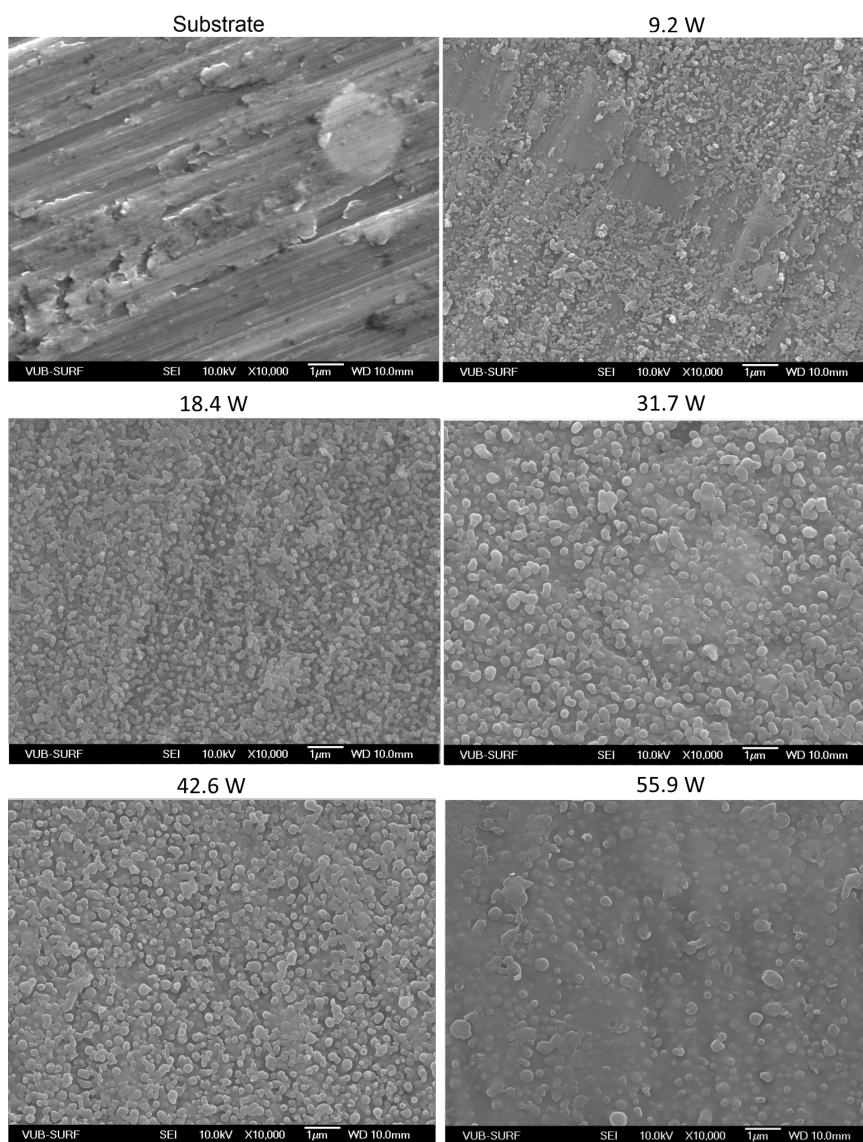
Figure 5: Low magnification (x10000) images of the surface of the deposited coatings.
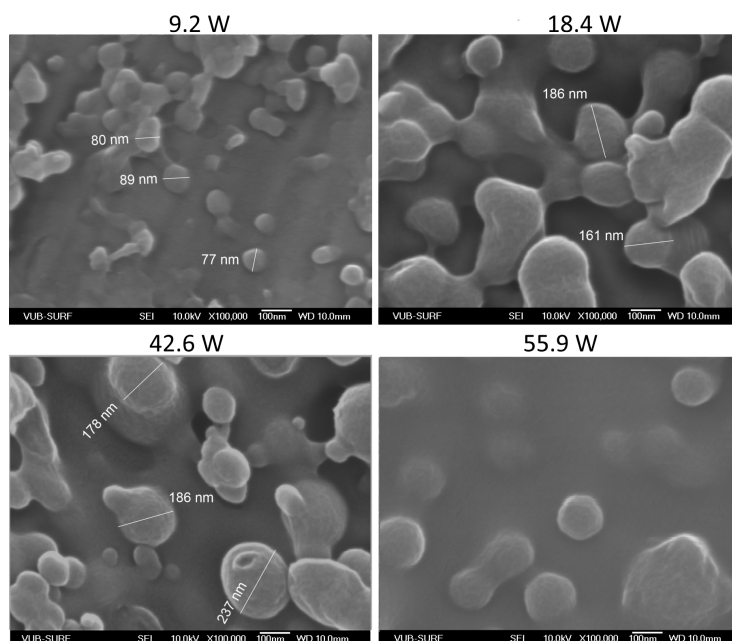
10

Figure 6: High magnification (x100k) images of the surface of the deposited coatings.

SEM, AFM confirms the presence of the features on the surface of the film. Moreover, it confirms the observations of SEM concerning the influence of the power/monomer feed to the morphology of the surface. The arithmetic average roughness (*Ra*) and the ten-point mean roughness (*Rz*) were also calculated. The *Ra* was estimated to be near 27 nm for all conditions and the *Rz* was estimated at 330 nm for coatings deposited with 8 W lowering to 200 nm for the rest of the deposition.

A model based on the observations of the morphology was used for the SE. Figure 8 shows the estimated thickness of the compact and the rough layer for different deposition parameters. The thickness of the compact layer and subsequently the deposition rates of the compact layer increases proportionally with the power. Higher deposition rates can be achieved when both *W* and *F* are increased proportionally. The thickness of the rough layer did not substantially vary, with the exception of the 55.9 W and was estimated between 100 nm and 150 nm. The thickness of this film is in all cases lower than the *Rz* values calculated by AFM. Since *Rz* indicates the valley to peak distance it is expected that the thickness of the rough layer should be around this value. The increase in the size of the sub-micron particles, which was observed by the SEM, re-

11

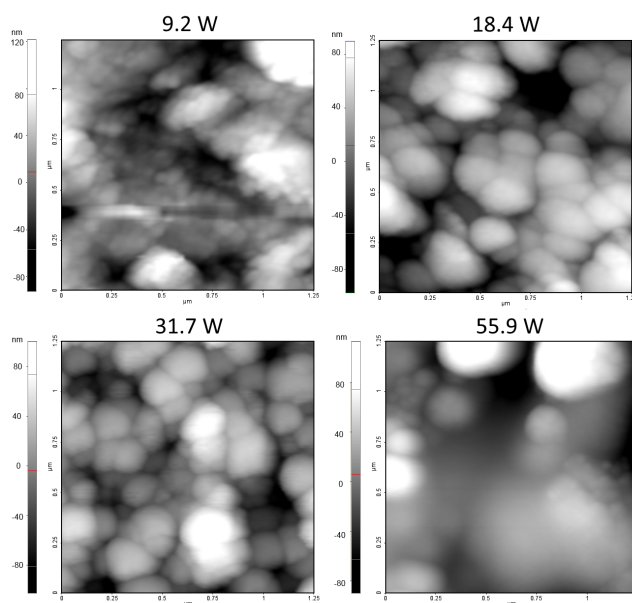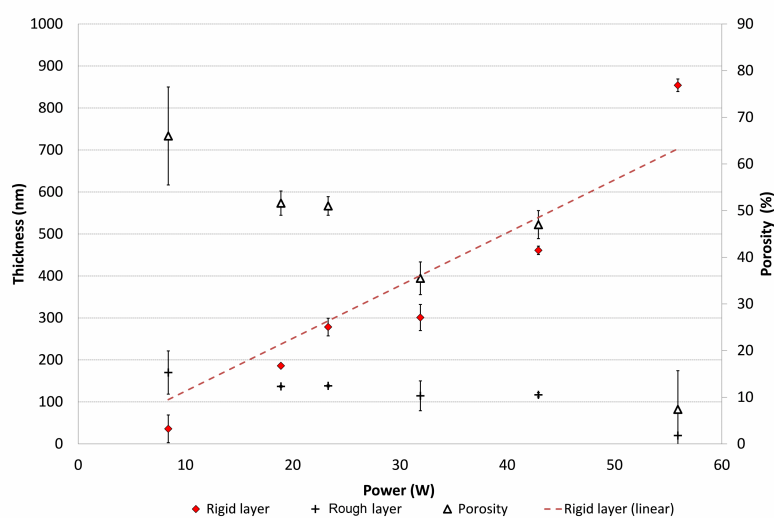Figure 7: AFM images of the surface topology for different deposition conditions.

Figure 8: Estimated thickness of the compact and the rough film, and percentage of voids in the porous film. W/FM parameter was the same for all depositions.

sults in a decrease in the empty space in the rough layer. It is practically diminished at 55.9 W where the sub-micron particles appear incorporated to the deposited coating.
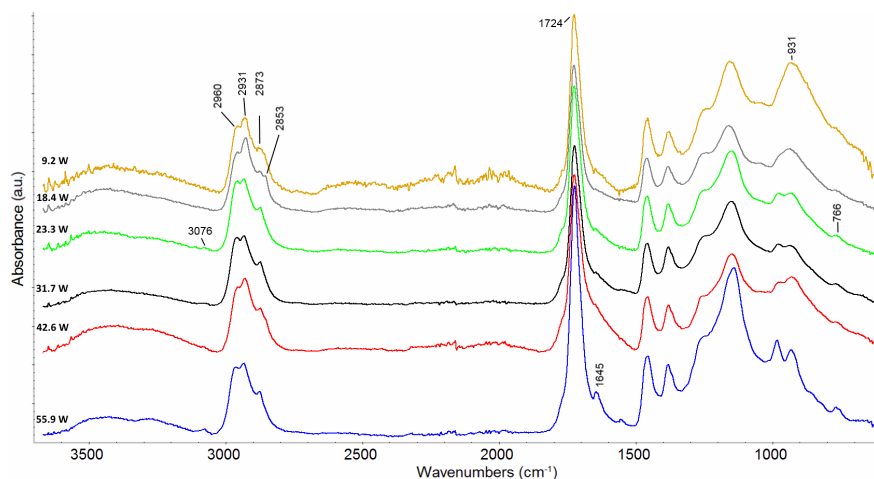
12

5.2   Study of the chemistry

Figure 9: FTIR absorbance spectra of coatings deposited with discharge power 9.2 W, 18.4 W, 23.3 W, 31.7 W, 42.6 W and 55.9 W and monomer feed adjusted to keep the W/FM parameter constant.

The infrared spectra of the deposited coatings are shown in fig. 9. The plasma polymer bands are broader than those of the conventional polymers revealing a higher degree of distribution of non-equivalent environments.[20] Several absorption bands are common for all the spectra. Among these, the principal are the $CH_{2/3}$ stretching (str) located in the region from $2800\,cm^{-1}$ to $3000\,cm^{-1}$, the strong absorption band that appears around $1724\,cm^{-1}$ which is characteristic for the ester group C=O str, the C−O str appearing near $1150\,cm^{-1}$ and $CH_{2/3}$ deformation vibrations at $1460\,cm^{-1}$ and $1380\,cm^{-1}$. A very weak peak at $3076\,cm^{-1}$ observed in the coatings deposited at 23 W, 31.7 W, 42.6 W and 55.9 W is assigned to CH_2 str vibrations of the residual C=C bonds. This indicates the presence of remaining unreacted allyl groups in the plasma coatings.[38–40] The presence of the unreacted allyl groups is confirmed by the presence of the doublet at $984\,cm^{-1}$ and $934\,cm^{-1}$ which is attributed to the wagging vibrations of the allyl functionalities. The Al_2O_3 absorption band falls also in the same region causing an overlap which makes the distinction of the allyl doublet difficult.[41] In the spectra of 9.2 W and 18.4 W, the single peak in that region is attributed to Al_2O_3 since there is no presence of a doublet and the complimentary peak at $3076\,cm^{-1}$ is missing.

13

In the spectra of the coatings of 23.3 W, 31.7 W and 42.6 W there is an overlap of both allyl doublet and Al_2O_3 band, while in the coating of 55.9 W only the allyl doublet appears. The C=C str absorption band near 1645 cm^{-1} which can barely be observed in the other spectra, confirms the presence of even higher concentrations of non-reacted allyl groups.

A weak band appears near 766 cm^{-1} in the coatings deposited with 23.3 W, 31.7 W and 42.6 W and is much stronger at 55.9 W. This peak is characteristic for poly(methyl methacrylate (MMA)) and is attributed to the rocking vibrations of the CH_2.[39] It is visible when long methylene chains are present and disappear in plasma polymers where the structure is more branched.[7] Its presence suggests a more linear and therefore less branched structure in the coatings deposited with high power and high monomer feed.

Table 2: Ratio of the area of C=O infrared bands (1665 cm^{-1} to 1850 cm^{-1}) to $CH_{2/3}$ bands (2750 cm^{-1} to 3100 cm^{-1}) of different pd-AMA coatings.

Power [W]	9.2	18.4	23.3	31.7	42.6	55.9
C=O:CH ratio	0.96	0.81	0.85	0.86	0.93	1.01

A comparison between the C=O str and the $CH_{2/3}$ str band provides a good indication of the retention of the ester functionality . The peak areas were calculated by estimating the integral of the spectrum from 1665 cm^{-1} to 1850 cm^{-1} for the C=O and from 2750 cm^{-1} to 3100 cm^{-1} for the $CH_{2/3}$ str, and linearly removing the background. Table 2 shows the ratios of the C=O str:$CH_{2/3}$ str band areas of the absorbance spectra of the plasma coatings deposited of fig. 9. The values of the C=O:$CH_{2/3}$ ratios are at the same level as those of coatings deposited in a different DBD reactor.[20] Apart from the 9.2 W deposition, there is an increase in the C=O:$CH_{2/3}$ ratio which indicates better retention of the ester group when coatings are deposited at high power and high monomer feed. The chemistry in the surface of the plasma coating is expected to be different from the rest of the coating with higher amounts of oxygen, due to several processes that take place after the deposition. When the thickness of the coating is relatively low, the global chemistry is also affected. That could justify the C=O:$CH_{2/3}$ ratio of the 9.2 W deposition. These changes in the concentration of ester functionali-
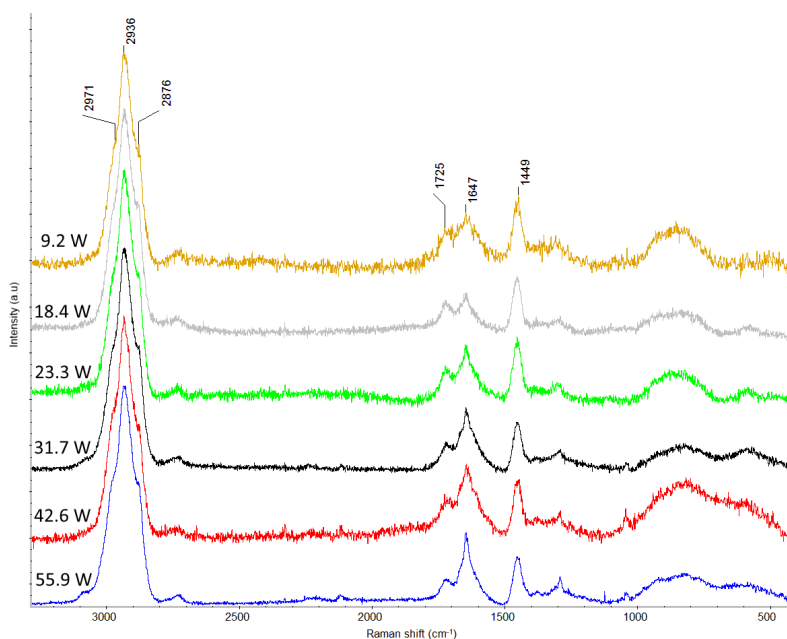
14

Figure 10: Raman spectra of coatings deposited with discharge power 9 W, 18 W, 23 W, 31.7 W, 42.6 W and 55.9 W and monomer feed and monomer feed adjusted to keep the W/FM parameter constant.

ties, even if they are not significant compared to the ones produced by different W/FM ratios, are still not negligible indicating a better retention of the ester functionality when higher power and monomer feed are used.

The Raman spectra of the deposited coatings are shown in fig. 10. The observed peaks have similar positions with the infrared spectra, however their intensity changes, as certain vibrations appear stronger either in the infrared or in the Raman spectra.[38,39] In the range between $2850 \, cm^{-1}$ to $3000 \, cm^{-1}$ several overlapping bands due to the vibrations of CH_x str are observed while their deformation vibrations appear near $1450 \, cm^{-1}$.[39,42] The C=O str vibration is less intense in the Raman spectra and falls at $1725 \, cm^{-1}$. The C=C str is found at $1647 \, cm^{-1}$. For the coating deposited with 9 W, the intensity of this band is relatively low and overlaps with the C=O str which makes the separation of the two peaks difficult. When the deposition takes place at higher powers and monomer feeds, the intensity of the peak clearly increases indicating a higher concentration of unreacted allyl groups in the coating.

This increase is more clearly seen by comparing the ratio between the C=C str and

Table 3: Ratio of the area of C=C bands ($1530\,\text{cm}^{-1}$ to $1688\,\text{cm}^{-1}$) to CH$_{2/3}$ bands ($2780\,\text{cm}^{-1}$ to $3150\,\text{cm}^{-1}$) of different pd-AMA coatings.

Power [W]	9.2	18.4	23.3	31.7	42.6	55.9
C=C:CH ratio	0.075	0.067	0.068	0.105	0.149	0.119

the CH$_\text{x}$ str bands. The peak areas were calculated by estimating the area of the spectrum from $1530\,\text{cm}^{-1}$ to $1688\,\text{cm}^{-1}$ for the C=C and from $2780\,\text{cm}^{-1}$ to $3150\,\text{cm}^{-1}$ for the CH$_\text{x}$ str and linearly removing the background. A partial overlap area with the C=O str is not expected to substantially alter the results. The C=O *str*:CH$_{2/3}$ *str* ratio increases when higher powers and monomer feeds are used, which confirms the observations of the infrared spectra (see table 3).

6 Conclusions

In this work, it was shown that the use of a constant W/FM parameter in the same plasma reactor could result in deposition of coatings with different morphology and chemistry when both discharge power and monomer feed are varied proportionally. This change of the deposition mechanism is mainly attributed to the transition of the plasma mode from pseudoglow discharge[43] to filamentary, due to the increase of the plasma density. The increase of both power and monomer flow also results in higher deposition rates, which in this case varied from $0.3\,\text{nm}\cdot\text{s}^{-1}$ to $5.7\,\text{nm}\cdot\text{s}^{-1}$.

The morphology of the coatings was substantially different when low power and monomer flow were used compared to those deposited at very high powers. More specifically, small particles were observed as features on the surface of the coatings. It appears that they interacted with the already deposited material and adhered to the coating. Their size increased with the increase in the power and the monomer flow by occupying higher amount of the surface and with a further increase in both parameters results they fuse into one rigid film.

The study of the chemistry showed a change of concentration of the allyl groups in the coatings. Moreover, an increase in the concentration of ester groups was observed at high powers and high monomer flows. This change, even not critical, was not expected

16

since it was previously shown that AMA retains its ester functionality better than n-Propyl methacrylate (nPMA) or PiB when the W/FM changes.[30,44] Therefore, for the same W/FM values, similar concentration of C=O groups would be expected.

It should be highlighted that when W/FM parameter is used in atmospheric pressure plasma, it does not take into consideration the type of the discharge, which affects the plasma deposition mechanism. The same W/FM parameter can result in films with different morphology, different thickness and a slight change in the chemistry due to the different type of plasma. It is therefore not recommended to use the W/FM parameter for non-homogeneous discharges however, it is important to mention that W/FM can be used under certain circumstances, for instance to compare the chemistry for different W or F when the other parameter is constant, it does not predict the deposited chemistry even in the same experimental setup.

References

[1] M. A. Lieberman and A. J. Lichtenberg, *Principles of plasma discharges and materials processing*, Cambridge Univ Press, 1994.

[2] R. Shishoo, *Plasma technologies for textiles*, CRC Press, 2007.

[3] A. Fridman, *Plasma chemistry*, Cambridge University Press, 2008.

[4] R. D'Agostino, P. Favia, C. Oehr and M. R. Wertheimer, *Plasma processes and polymers*, Wiley Online Library, 2005.

[5] D. Merche, N. Vandencasteele and F. Reniers, *Thin Solid Films*, 2012, **520**, 4219–4236.

[6] C. Tendero, C. Tixier, P. Tristant, J. Desmaison and P. Leprince, *Spectrochim. Acta B*, 2006, **61**, 2–30.

[7] J. Friedrich, *Plasma Processes Polym.*, 2011, **8**, 783–802.

[8] J. Friedrich, R. Mix and G. Kühn, *Surf. Coat. Technol.*, 2005, **200**, 565–568.

17

[9] F. S. Denes and S. Manolache, *Prog. Polym. Sci.*, 2004, **29**, 815–885.

[10] H. Yasuda, *J. Polymer Sci.: Macromolecular Reviews*, 1981, **16**, 199–293.

[11] J. D. Whittle, R. D. Short, D. A. Steele, J. W. Bradley, P. M. Bryant, F. Jan, H. Biederman, A. A. Serov, A. Choukurov and A. L. Hook, *Plasma Processes Polym.*, 2013, **10**, 767–778.

[12] H. K. Yasuda, *Plasma Processes and Polymers*, 2005, **2**, 293–304.

[13] R. Morent, N. De Geyter, T. Jacobs, S. Van Vlierberghe, P. Dubruel, C. Leys and E. Schacht, *Plasma Processes and Polymers*, 2009, **6**, S537–S542.

[14] N. De Geyter, R. Morent, S. Van Vlierberghe, P. Dubruel, C. Leys, L. Gengembre, E. Schacht and E. Payen, *Prog. Org. Coat.*, 2009, **64**, 230–237.

[15] M. Tatoulian, F. Arefi-Khonsari, L. Tatoulian, J. Amouroux and J. Borra, *Chemistry of materials*, 2006, **18**, 5860–5863.

[16] M. Bashir, J. M. Rees and W. B. Zimmerman, *Surface and Coatings Technology*, 2013, **234**, 82–91.

[17] T. C. Tsai and D. Staack, Plasma Science, 2010 Abstracts IEEE International Conference on, 2010, pp. 1–1.

[18] M. Asandulesa, I. Topala, V. Pohoata and N. Dumitrascu, *Journal of Applied Physics*, 2010, **108**, 093310.

[19] C. Amorosi, T. Fouquet, V. Toniazzo, D. Ruch, L. Averous, V. Ball and M. Michel, *Reactive and Functional Polymers*, 2012, **72**, 341–348.

[20] A. Kakaroglou, G. Scheltjens, B. Nisol, I. De Graeve, G. Van Assche, B. Van Mele, R. Willem, M. Biesemans, F. Reniers and H. Terryn, *Plasma Processes Polym.*, 2012, **9**, 799–807.

[21] J. Petersen, R. Bechara, J. Bardon, T. Fouquet, F. Ziarelli, L. Daheron, V. Ball, V. Toniazzo, M. Michel, A. Dinia *et al.*, *Plasma Processes and Polymers*, 2011, **8**, 895–903.

[22] J. Kriegseis, B. Möller, S. Grundmann and C. Tropea, *J. Electrostat.*, 2011, **69**, 302–312.

[23] T. Manley, *Transactions of the electrochemical society*, 1943, **84**, 83–96.

[24] G. Nersisyan and W. Graham, *Plasma Sources Science and Technology*, 2004, **13**, 582.

[25] E. D. Palik, *Handbook of optical constants of solids*, Academic press, 1998, vol. 3.

[26] T. Lichtenstein, *Handbook of thin film materials*, College of Engineering and Applied Science, University of Rochester, 1979.

[27] D. Aspnes, *Thin Solid Films*, 1982, **89**, 249–262.

[28] G. A. Niklasson, C. Granqvist and O. Hunderi, *Appl. Opt.*, 1981, **20**, 26–30.

[29] B. Nisol, A. Batan, F. Dabeux, A. Kakaroglou, I. De Graeve, G. Van Assche, B. Van Mele, H. Terryn and F. Reniers, *Plasma Processes Polym.*, 2013, **10**, 564–571.

[30] A. Batan, B. Nisol, A. Kakaroglou, I. De Graeve, G. Van Assche, B. Van Mele, H. Terryn and F. Reniers, *Plasma Processes Polym.*, 2013.

[31] U. Kogelschatz, *Plasma Chem. Plasma Process.*, 2003, **23**, 1–46.

[32] N. Gherardi, G. Gouda, E. Gat, A. Ricard and F. Massines, *Plasma Sources Sci. Technol.*, 2000, **9**, 340.

[33] H. Conrads and M. Schmidt, *Plasma Sources Sci. Technol.*, 2000, **9**, 441.

[34] A. Bouchoule, *Phys. World*, 1993, **6**, 47–51.

[35] H. Kersten, G. Thieme, M. Fröhlich, D. Bojic, D. Tung, M. Quaas, H. Wulff and R. Hippler, *Pure Appl. Chem.*, 2005, **77**, 415–428.

[36] C. Hollenstein, *Plasma Phys. Controlled Fusion*, 2000, **42**, R93.

[37] S. Letts, D. Myers and L. Witt, *J. Vac. Sci. Technol.*, 1981, **19**, 739–742.

[38] D. W. Mayo, F. A. Miller and R. W. Hannah, *Course notes on the interpretation of infrared and Raman spectra*, John Wiley and Sons, New York, 2004.

[39] G. Socrates, *Infrared and Raman characteristic group frequencies: tables and charts*, John Wiley and Sons, New York, 2001.

[40] M. H. Jamróz, M. E. Jamróz, J. E. Rode, E. Bednarek and J. C. Dobrowolski, *Vib. Spectrosc.*, 2009, **50**, 231–244.

[41] A. J. Maeland, R. Rittenhouse, W. Lahar and P. V. Romano, *Thin Solid Films*, 1974, **21**, 67–72.

[42] H. Willis, V. Zichy and P. Hendra, *Polymer*, 1969, **10**, 737–746.

[43] R. Bartnikas, *Journal of Applied Physics*, 1969, **40**, 1974–1976.

[44] B. Nisol, G. Arnoult, T. Bieber, A. Kakaroglou, I. De Graeve, G. Van Assche, H. Terryn and F. Reniers, *Plasma Processes and Polymers*, 2014, **11**, 335–344.

The plasma density influences the chemistry and the morphology of the deposited plasma polymers even under the same energy to monomer ratio.